

# The physical properties of two potential targets for space missions: (155140) 2005 UD and (612267) 2001 SG286

R. M. Gherase,<sup>1,2,3★</sup> M. Popescu<sup>1b</sup>,<sup>1,2,3★</sup> O. Vaduvescu,<sup>1,4,5</sup> T. G. Wilson,<sup>4</sup> J. de León<sup>1b</sup>,<sup>5,6</sup> V. Lorenzi,<sup>5,7</sup> J. Licandro<sup>1b</sup>,<sup>5,6</sup> D. Morate,<sup>5,6</sup> G. Simion,<sup>2</sup> A. Aznar Macías<sup>8</sup> and B. A. Dumitru<sup>9</sup>

<sup>1</sup>University of Craiova, Alexandru Ioan Cuza 13, Craiova 200585, Romania

<sup>2</sup>Astronomical Institute of the Romanian Academy, 5 Cușitul de Argint, 040557 Bucharest, Romania

<sup>3</sup>Astroclubul București, Blvd Lascăr Catargiu 21, 10663 Bucharest, Romania

<sup>4</sup>Isaac Newton Group of Telescopes (ING), Apto. 321, E-38700 Santa Cruz de la Palma, Canary Islands, Spain

<sup>5</sup>Instituto de Astrofísica de Canarias (IAC), C/Vía Láctea s/n, E-38205 La Laguna, Spain

<sup>6</sup>Departamento de Astrofísica, Universidad de La Laguna, , E-38205, La Laguna, Spain

<sup>7</sup>Fundación Galileo Galilei – INAF, Rambla José Ana Fernández Pérez 7, E-38712 Breña Baja, Spain

<sup>8</sup>Isaac Aznar Observatory, Alculbas, Valencia, Spain

<sup>9</sup>Institute of Space Science (ISS), 409 Atomiștilor Street, 077125 Bucharest, Romania

Accepted 2024 October 21. Received 2024 October 21; in original form 2024 February 16

## ABSTRACT

The ground-based characterization of asteroids is a key step for planning their exploration. The near-Earth asteroid 155140 (2005 UD) is a potential flyby target of Japan Aerospace Exploration Agency’s *DESTINY+* (*Demonstration and Experiment of Space Technology for INterplanetary voYage with Phaethon fLyby and dUst Science*) mission, while (612267) 2001 SG286 has been considered as a possible target for *in-situ* exploration. We aim to determine their physical properties using the observations obtained with various telescopes from Canary Islands Observatory. For 2005 UD, we confirmed the two peak light curve, a rotation period of  $5.224 \pm 0.003$  h and an amplitude of 0.34 mag. However, a three peak solution seemed also to fit the light curve, but this was discarded as implausible. Using the obtained visible to near-infrared spectrum we classified it as a Cb type, and we found a spectral matching with heated carbonaceous chondrite meteorites of CM2 type. The thermal emission flux at  $2.2 \mu\text{m}$  points to an albedo of  $p_V = 0.06 \pm 0.02$ . There are significant differences in the spectrum of 2005 UD compared to that of (3200) Phaeton, hypothesized as its parent body. The accurate visible spectrum obtained with the Gran Telescopio Canarias indicate that 2001 SG286 is an S-type asteroid. The photometric data obtained with Isaac Newton Telescope suggest a rotation period of  $12.30 \pm 0.01$  h and an amplitude of 0.64 mag. With these observations we found its absolute magnitude  $H = 21.4 \pm 0.3$ , and estimate its size as  $160 \pm 45$  m.

**Key words:** methods: observational – techniques: imaging spectroscopy – minor planets, asteroids: individual: 2005 UD, 2001 SG286.

## 1 INTRODUCTION

The study of near-Earth asteroids (NEAs) is important as these bodies can reveal a plethora of information about the origin and history of our planetary system. For the practical means they can serve as *in-situ* resources in the near future. This is why the NEAs have become important targets for the space exploration. For a part of them, the current technologies allow both a flyby and a sample-return mission, thanks to their accessibility in terms of  $\Delta V$  budget.

Moreover, those which make threatening close approaches to Earth are classified as potentially hazardous asteroids and they may represent a threat for our world. Thus, it is not surprising that over the past couple of decades substantial observational work has been undertaken to understand this population of small bodies. The observations performed using ground-based telescopes can provide

information such as rotation period, size, and shape of the asteroid from light-curve analysis, whereas spectroscopy offers the ability to probe surface composition from taxonomic studies.

Whilst ground-based observations can allow the study of many properties of NEAs, *in-situ* observations from a flyby or orbiting spacecraft can reveal knowledge that is either difficult or impossible to obtain remotely. This is evident in the recent missions such as JAXA (Japan Aerospace Exploration Agency)/Hayabusa2 (e.g. Nakamura et al. 2023) and NASA/OSIRIS-REx - Origins Spectral Interpretation Resource Identification Security Regolith Explorer (e.g. Lauretta et al. 2019) that have greatly improved the understanding of these objects.

Planning for space exploration requires detailed ground-based observations. Therefore, we aim to make a detailed characterization of the NEAs (155140) 2005 UD (hereafter 2005 UD) and (612267) 2001 SG286 (hereafter 2001 SG286), which represent possible targets for future spacecraft exploration.

\* E-mail: [radu.gherase@gmail.com](mailto:radu.gherase@gmail.com) (RMG), [popescu.marcel@ucv.ro](mailto:popescu.marcel@ucv.ro) (MP)

**Table 1.** Summary of photometric and spectroscopic observations of 2005 UD. The observer-target distances,  $\Delta$ , heliocentric distances,  $r$ , and phase angles,  $\alpha$ , are taken from the JPL HORIZONS database, accessed on 2024 January 25.

Date	UT	$\Delta$ (au)	$\alpha$ (deg)	$r$ (au)	Airmass	Exp. time (s)	Filter/ $\lambda_{\text{range}}$ ( $\mu\text{m}$ )	Telescope	Instrument
Photometry									
2018-10-14	23:05–04:29	0.354–0.357	3.99–4.42	1.35–1.35	1.08–1.95	395×30	Sloan <i>r</i>	INT	WFC
2018-10-15	21:18–03:05	0.367–0.370	5.71–6.15	1.36–1.37	1.08–1.54	96×40	Sloan <i>g</i>		
	21:01–03:01	0.367–0.370	5.69–6.14	1.36–1.36	1.08–1.66	100×30	Sloan <i>r</i>		
	21:24–03:03	0.367–0.370	5.72–6.15	1.36–1.36	1.08–1.50	96×40	Sloan <i>i</i>		
2018-10-10	21:37–23:34	0.301–0.302	5.3–5.1	1.30–1.30	1.94–1.19	82×30	Sloan <i>r</i>	TAR2	FLI KL400
2018-10-11	21:48–00:48	0.313–0.315	2.8–2.5	1.31–1.31	1.66–1.08	160×45	Sloan <i>r</i>		
2018-10-15	20:10–22:09	0.366–0.367	5.6–5.8	1.36–1.36	2.36–1.30	116×30	Sloan <i>r</i>		
2018-10-16	02:29–04:57	0.370–0.372	6.1–6.3	1.36–1.37	1.25–2.78	152×30	Sloan <i>r</i>		
Spectroscopy									
2018-10-17	23:37–03:36	0.398–0.401	9.23–9.49	1.39–1.39	1.09–1.67	17×600	0.4–1.0	INT	IDS
2018-10-26	01:20–02:22	0.531–0.531	18.81–18.85	1.48–1.48	1.37–1.65	2×1800	0.4–1.0		
2018-10-29	23:45–01:34	0.601–0.602	21.89–21.95	1.53–1.53	1.14–1.50	1×560, 3×1800	0.4–1.0		
2018-10-31	21:44–23:07	0.636–0.637	23.13–23.16	1.55–1.55	1.09–1.11	36×90	0.8–2.5	TNG	NICS

For instance, JAXA has proposed recently the *Demonstration and Experiment of Space Technology for INterplanetary voYage with Phaethon fLyby and dUst Science (DESTINY+)* mission to visit the NEAs (3200) Phaethon and 2005 UD, planned for launch in 2024 with flybys of these objects nominally occurring 2–3 yr later (Ozaki et al. 2022). Phaethon, the main target of *DESTINY+* and the source of the Geminids meteor shower, is dynamically believed to be the parent body of 2005 UD following a splitting event (Ohtsuka et al. 2006; Kasuga 2009; Ryabova, Avdyushev & Williams 2019).

However, compared to Phaethon, less is known about 2005 UD. Previous photometric studies have resolved the rotation period to  $P = 5.23\text{--}5.25$  h, with colour observations of 2005 UD indicating a bluish surface similar to Phaethon (Jewitt & Hsieh 2006; Kinoshita et al. 2007). Using NEOWISE (Near-Earth Object Wide-field Infrared Survey Explorer) photometry and thermophysical models, a diameter of  $1.2\pm 0.4$  km and a geometric albedo of  $0.14\pm 0.09$  has been determined (Masiero, Wright & Mainzer 2019). In addition, by using the albedo–polarization relation, Devogèle et al. (2020) determined a diameter of  $1.3\pm 0.1$  km and geometric albedo value of  $0.10\pm 0.02$ . While spectroscopic observations have previously been taken for Phaethon, no such observations in the near-infrared have been published for 2005 UD to date. Phaethon has been classified as a B type (Licandro et al. 2007). Therefore, additional spectroscopy of 2005 UD is needed to compositionally identify the body and potentially link it to Phaethon, whereas additional multiband photometry can help confirm and refine previously determined rotation properties and colour indices.

Furthermore, we aim to make a detailed characterization of the Apollo asteroid 2001 SG286, which was considered for several sample-return missions to a D-type asteroid. The existing spectral data (Binzel et al. 2004; Popescu et al. 2011) indicate a possible D-type peculiar composition. The origin of these objects, their evolution and the mineralogy remains poorly known. They could be rich in primordial organics and could be related to comets (Barucci et al. 2018). The NEAs with a D-type composition generally represent rare targets and so far no spacecraft has ever visited one. Thus, 2001 SG286 was chosen as the baseline target for the MarcoPolo-2D mission proposal.<sup>1</sup> It may still represent a possible target for a sample-

return mission, as the estimated  $\Delta V$  budget for it is  $5.6 \text{ km s}^{-1}$ . However, before establishing this goal, more observations are needed to clarify its nature. We therefore made detailed observations to this object during its favourable apparition in 2020 October using some of the large telescopes from the Canary Islands.

The article is organized as follows: Section 2 describes the photometric and the spectroscopic observations and the instruments we used to perform them, Section 3 summarizes the methods applied for the data reduction, the results are presented in Section 4, and the conclusions are shown in Section 5.

## 2 OBSERVATIONS

We obtained photometric observations with the 0.46 m Telescopio Abierto Remoto (TAR2) and with the 2.54 m Isaac Newton Telescope (INT). The spectra of 2005 UD were obtained with the INT in the visible range and with the 3.58 m Telescopio Nazionale Galileo (TNG) over the near-infrared wavelengths. Because of its faint apparent magnitude we could acquire only the visible spectrum of 2001 SG286 with the 10.4 m Gran Telescopio Canarias (GTC). We acquired data in 2018 October for 2005 UD, and in 2020 October for 2011 SG286, during their most recent close approaches. The INT, TNG, and GTC telescopes are located at the El Roque de Los Muchachos Observatory, on the island of La Palma (Canary Islands, Spain). TAR2 is located at Teide Observatory, on the island of Tenerife (Canary Islands, Spain). The observational logs are shown in Tables 1 and 2. Below we describe the setups used for our observations.

The opportunity to characterize these targets occurs about once every decade with a visibility window of few weeks. The following time intervals when these objects can be photometrically and spectroscopically observed are during 2028 October for 2005 UD, and during 2028 May for 2001 SG286. They were found by constraining the apparent  $V$  magnitude to be less than  $V \approx 20$  and the solar elongations larger than  $\epsilon \approx 60^\circ$ .

### 2.1 Photometry

We used the Wide Field Camera’s CCD4 mounted on the 2.54 m aperture INT, and equipped with Sloan photometric filters for imaging both targets. We used a subframe of  $1821 \times 1821$  pixels, with

<sup>1</sup><https://stem.open.ac.uk/research-project/marcopolo/overview/marcopolo-2d> accessed on 2023 October 02.

**Table 2.** Summary of photometric and spectroscopic observations of 2001 SG286. The observer-target distances,  $\Delta$ , heliocentric distances,  $r$ , and phase angles,  $\alpha$ , are taken from the JPL HORIZONS database.

Date	UT	$\Delta$ (au)	$\alpha$ (deg)	$r$ (au)	Airmass	Exp. time (s)	Filter/ $\lambda_{\text{range}}$ ( $\mu\text{m}$ )	Telescope	Instrument
Photometry									
2020-10-07	23:49–03:36	0.152–0.152	40.2–39.9	1.11–1.11	1.06–1.59	208×50	Sloan $r$	INT	WFC
2020-10-09	00:32–04:27	0.155–0.156	38.4–38.1	1.12–1.12	1.07–1.94	222×50	Sloan $r$		
2020-10-10	00:31–04:27	0.159–0.159	36.7–36.5	1.12–1.12	1.06–1.99	223×50	Sloan $r$		
2020-10-10	20:57–23:52	0.162–0.162	35.4–35.2	1.13–1.13	1.04–1.21	150×50	Sloan $r$		
2020-10-12	02:00–04:21	0.166–0.167	33.6–33.5	1.13–1.13	1.19–1.94	125×50	Sloan $r$		
2020-10-25	20:52–02:40	0.235–0.237	22.6–22.5	1.21–1.21	1.00–1.46	157×120	Sloan $r$		
2020-10-26	19:26–03:12	0.241–0.243	22.4–22.4	1.21–1.21	1.00–1.70	210×120	Sloan $r$		
2020-10-27	19:48–03:50	0.247–0.250	22.3–22.3	1.22–1.22	1.00–2.20	210×120	Sloan $r$		
2020-10-28	19:42–03:14	0.254–0.256	22.3–22.3	1.22–1.23	1.00–1.78	158×150	Sloan $r$		
Spectroscopy									
2020-10-08	01:29–02:00	0.152–0.152	40.0–40.0	1.11–1.11	1.15–1.19	3×600	0.5–0.95	GTC	OSIRIS

a field of view of  $10.14 \times 10.14$  arcmin and  $0.33$  arcsec pixel $^{-1}$ . The fast readout mode was set resulting in a readout time of 18 s per exposure. The NEAs were tracked differentially using half of the proper motions retrieved from the Minor Planet Center (MPC) ephemeris service at the observing moment.

The 2005 UD observations were taken during two consecutive nights, 2018 October 14 and 15. On the first night, we observed 5.4 h in the Sloan  $r$  filter with an exposure time of 30 s yielding a cadence of 48 s and 395 frames. During the second night, observations were taken cycling through Sloan  $g$ ,  $r$ , and  $i$  filters with exposure times of 40, 30, and 40 s, respectively, resulting in a typical cadence between images in the same filter of 193 s for a total of 6.0 h observing time. Whilst this gives a coarser sample of the rotational light curve compared to the previous night, the data obtained on the three bands allow for analysis of the asteroid colour as a function of rotation period.

The data for 2001 SG286 was captured during two successive observing runs, five nights from October 7 to 13 and four nights from October 25 to 28 during the 2020 approach. As 2001 SG286 was a more challenging target due to its faint magnitude, the observing strategy in this case consisted in continuous image acquisition through the Sloan  $r$  filter during several hours as long as the asteroid was in a favourable position for observation. Depending on the target’s apparent magnitude and the general sky conditions, the individual exposures were set between 50–120 s long, for a minimum target signal to noise ratio (SNR) of 10.

We used the TAR2 telescope from the Instituto de Astrofísica de Canarias to complete our 2005 UD light-curve analysis. It has  $f/D = 2.8$  at the prime focus, and it is equipped with a FLI-Kepler KL400 camera. The instrument is a back illuminated  $2K \times 2K$  pixels CMOS (complementary metal–oxide–semiconductor) with a pixel size of  $11 \mu\text{m}^2$ . The plate scale is  $1.77$  arcsec pixel $^{-1}$  and the field of view is  $\sim 1$ deg $^2$ .

## 2.2 Visible spectroscopy

The asteroid 155140 (2005 UD) was observed spectroscopically in the optical range using the Intermediate Dispersion Spectrograph (IDS) mounted on the INT. We used the low-resolution grating R150V with the blaze wavelength set at  $0.65 \mu\text{m}$ . Considering the typical seeing between  $0.6$ – $1.5$  arcsec, the slit with  $1.5$  arcsec width was chosen. The telescope worked in the differential tracking

mode assisted with manual adjustments for keeping the target in the slit. The apparent movement rates were retrieved from the MPC website.

The exposures were taken using the EEV10 CCD that has a scale of  $0.40$  arcsec pixel $^{-1}$ . A binning of  $1 \times 1$  was used and the CCD readout speed was set to slow. This setup yields a spectrum that covers a wavelength range of  $0.4$ – $1.0 \mu\text{m}$  and a resolving power of  $R \sim 750$ . It should be noted that EEV10 sensor used in this case is optimized for the blue spectral range and at wavelengths longer than  $0.85 \mu\text{m}$  the fringing significantly decrease the SNR of the data.

The spectra of 2005 UD were obtained with the slit aligned with the parallactic angle. On the first observational epoch 17 exposures of 600 s each were taken over a 4-h interval with an average cadence of 0.23 h. Subsequently, two and three spectra with integration times of 1800 s each were obtained on the second and third nights, respectively, with an additional 560 s exposure taken on October 29. This observational strategy allows for the study of any changes in the spectra over the rotation period of the asteroid and for the different phase angles of the target obtained over the multiple nights.

During each observational night three spectra of four G2V solar analogue stars were taken using the same instrumental setup described above. This was done in order to obtain reflectance spectra of the asteroid by dividing the observations of 2005 UD by the average solar analogue spectra for each night. We used the following G2V stars HD 19999, HD 27089, and HD 5495.

Because 2001 SG286 was a much fainter target, we used the GTC equipped with Optical System for Imaging and low Resolution Integrated Spectroscopy (OSIRIS) instrument (Cepa et al. 2000; Cepa 2010) for acquiring its visible spectrum. This instrument had two Marconi CCD detectors, each with  $2048 \times 4096$  pixels and a total unvignetted field of view of  $7.8 \times 7.8$  arcmin. We used the  $1.2$  arcsec slit and the R300R grism (resolution  $R = 348$  for a  $0.6$  arcsec slit, dispersion of  $7.74 \text{ \AA pixel}^{-1}$ ) covering the  $0.48$ – $0.92 \mu\text{m}$  wavelength range. The R300R grism is used in combination with a second-order spectral filter. The slit was oriented along the parallactic angle to minimize the effects of atmospheric differential refraction and the telescope tracking was set at the asteroid proper motion. A number of three exposures of 600 s each were obtained on the night of October 7 when the asteroid had an apparent  $V$  magnitude of 18.6. For calibration purposes, we obtained the spectra of two solar analogues, namely SA 93–101 and SA 98–978.

### 2.3 Near-infrared spectroscopy

The near-infrared spectrum of 2005 UD was obtained with TNG telescope on the night of 2018 October 31 when the asteroid had the apparent magnitude 18.5. We used the Near Infrared Camera Spectrometer (NICS) with the Amici prism disperser (Baffa et al. 2001). The NICS instrument has an Hg–Cd–Te Hawaii 1024 × 1024 array with a pixel scale of 0.25 arcsec pixel<sup>-1</sup>. This setup yields wavelength coverage of 0.8–2.5 μm and a resolving power  $R \approx 50$ .

During the observations the seeing varied in the range 0.7–1.0 arcsec and therefore a slit width of 1.5 arcsec was chosen. On 2018 October 31, 36 exposures of 90 s each were taken over 1.4 h in an ABBA nodding pattern, thus resulting in nine cycles, with a 10 arcsec offset between the A and B positions. The observations were taken with the slit oriented at the parallactic angle while the telescope tracking differentially at the proper motion of the asteroid. Solar analogues Land112-1333, Land115-271, and Land93-101 were observed at the same epoch using the same setup in order to determine the relative reflectance of the asteroid.

## 3 DATA REDUCTION

At the beginning and at the end of each observing session we acquired the calibration frames, bias, and flat field. For the photometric observations, we obtained sky flats during the twilight. The flats for the spectroscopic data were acquired with the lamp available at each instruments. We applied these standard corrections using the Image Reduction and Analysis Facility (IRAF) packages (Tody 1986). Then, the data reduction was performed according to the type of each observations.

### 3.1 Photometry

Analysis of asteroid light curves can be a powerful tool in obtaining physical information of body. By establishing the periodicity and amplitude of the light curve it is possible to determine the size, shape, and potentially irregularities or binarities of asteroids.

The photometric data were reduced using two well-known software packages, namely the Photometry Pipeline – PP (Mommert 2017), and the MPO CANOPUS.<sup>2</sup> All the chosen reference stars have a magnitude uncertainty of less than 0.01 mag. The nightly zero-points were found to be consistent up to  $\approx 0.1$  mag.

PP is software package written in PYTHON which produces calibrated photometry from the FITS images by performing the astrometric registration, aperture photometry, photometric calibration, and asteroid identification. It uses the Astromatic suite,<sup>3</sup> namely SExtractor for source identification and aperture photometry (Bertin & Arnouts 1996), SCAMP for astrometric calibration (Bertin 2006), and SWARP for image regridding and co-addition (Bertin et al. 2002). It also uses the Jet Propulsion Laboratory (JPL) HORIZONS module for obtaining the Solar system objects ephemeris in order to identify them in the images. For astrometric registration, we used the GAIA catalogue (Gaia Collaboration 2018). The PanSTARRS (Panoramic Survey Telescope and Rapid Response System) catalogue (Flewelling et al. 2020) was used for all photometric calibration. PP uses aperture photometry performed by Source Extractor. The PP algorithm that finds the optimum aperture radius based on a curve-of-growth analysis (Howell 2000) was applied. This was used with the default parameters, namely ‘the smallest aperture radius at

which at least 70 percent of each of the total target flux and the total background flux is included and at the same time the difference between the normalized target and background flux levels is smaller than 5 percent’ (Mommert 2017).

MPO CANOPUS is a complete package for astrometry, photometry, and light-curve inversion techniques.<sup>4</sup> It was developed by Brian D. Warner since 1999 and it is a research-level tool for amateurs, small colleges, and professionals. This software package processes data from the FITS images by performing the astrometric registration, aperture photometry, photometric calibration, and asteroid identification.

Finally, MPO CANOPUS was also used for the rotation period analysis, using the Fourier Analysis of Light Curves algorithm proposed by Harris et al. (1989). The light-curve plots are shown in Figs 1 and 2. The Reduced Magnitude on the  $Oy$ -axis represents the Sloan filter magnitude values that have been corrected from sky magnitudes to unity distance by applying  $-5\log(\Delta r)$  to the initial measurements, where  $\Delta$  is the Earth-asteroid distance and  $r$  is the Sun-asteroid distance. The  $Ox$ -axis represents the rotational phase.

### 3.2 Spectroscopy

To obtain the reflectance as a function of wavelength the data reduction of spectral exposures is required. The standard procedures specific to each instrument were employed. After the image pre-processing (bias and flat-field corrections), these routines include the following steps, tracing the spectrum in the exposures, extraction of flux values as a function of pixel position, combining the data from the multiple images corresponding to the same object, and wavelength calibration.

The final step provides the reflectance spectra by dividing the asteroid observed spectrum with the G2V solar analogues one, and then normalizing it. We acquired nearby solar analogue star spectra in every observing session for each target, as following: HD5495, HD19999, and HD27089 for the 2005 UD spectrum and SA93-101 and SA98-978 for 2001 SG286. All spectra were normalized to 0.55 μm.

For the INT spectral observations, the GNU OCTAVE software package (Eaton et al. 2015) was used to generate scripts for IRAF, to perform these tasks automatically. The extraction of the raw spectrum from the images was made with the *apall* package. Each image was visually inspected to avoid artefacts such as contamination due to background stars, target tracking errors, or spurious reflections (in case of targets located in the apparent vicinity of the Moon). The wavelength calibration was made based on the images of a CuAr + CuNe lamp (Popescu et al. 2019).

The spectrum of 2001 SG286 obtained with GTC was obtained with a Matlab dedicated routine (Morate et al. 2016). The sky background was subtracted and a one-dimensional spectrum was extracted using a variable aperture, corresponding to the pixel where the intensity was 10 percent of the peak value. Wavelength calibration was carried out using Xe+Ne + HgAr lamps.

Because of the sky brightness in the near-infrared, the data reduction of the TNG/NICS observations includes additional steps (Medeiros et al. 2019). After the image pre-processing, we subtracted the consecutive A and B images and then extracted the one-dimensional spectrum from each A–B pair. Wavelength calibration was made using a look-up table of the theoretical dispersion predicted by ray-tracing and adjusted to fit observed telluric absorptions. These

<sup>2</sup><https://minplanobs.org/BdwPub/php/displayhome.php>

<sup>3</sup><https://www.astromatic.net/>

<sup>4</sup><https://minplanobs.org/BdwPub/php/mpocanopus.php>

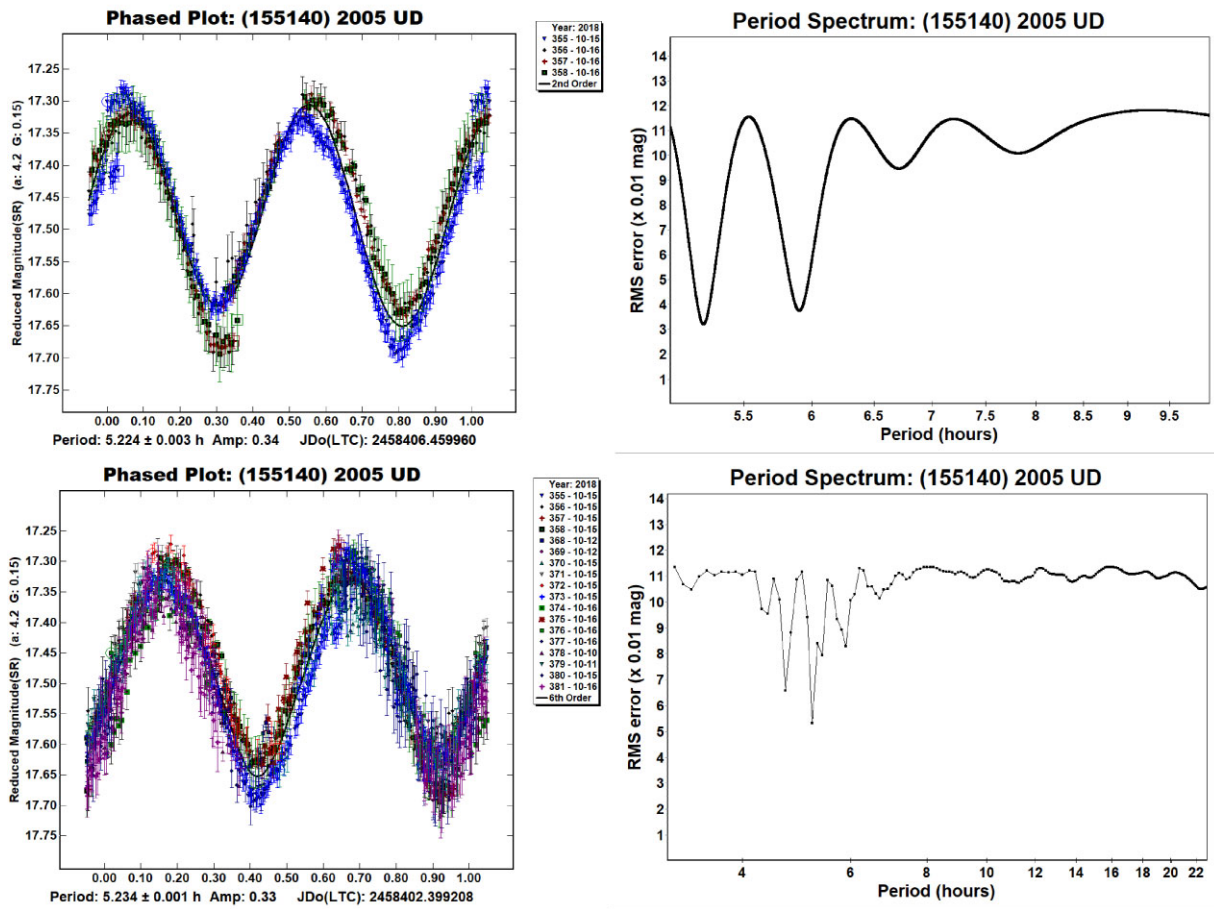


**Figure 1.** The light curves of 2005 UD (left) and their corresponding periodograms (right). The various observing sessions are plotted with a different colour. The selected periods represent the solutions reported in the paper. On top is the second-order polynomial fit using the INT data exclusively, on the bottom is the sixth-order polynomial fit using the INT data combined with the TAR telescopes and ALCDEF data.

tasks were done using a specific program in PYTHON provided by the telescope staff.

In the case of 2005 UD, in order to create a more complete profile for detailed analysis, we merged the near-infrared with the visible spectral data by using a data minimization procedure in the overlapping spectral region 0.8–0.85  $\mu\text{m}$  which consisted in normalizing the visible data to reduce as much as possible the mean square error between the two spectra in the respective interval.

## 4 RESULTS AND DISCUSSIONS

We present the photometric, spectrophotometric, and spectroscopic properties of these two NEAs. These are discussed in the context of previous published results. While the previous data indicated two bodies with carbonaceous chondrite like composition (Binzel et al. 2004; Jewitt & Hsieh 2006), the spectrum found for 2001 SG286 indicates an ordinary chondrite-like composition. Thus, this section is divided in two parts corresponding to each object.

### 4.1 (155140) 2005 UD

*The light curves.* We combined the INT/WFC (Wide Field Camera) photometry with the data obtained with 46-cm TAR robotic telescopes, and with the archival data from Asteroid Lightcurve Data

Exchange Format<sup>5</sup> (ALCDEF) database, namely those obtained by Warner & Stephens (2019).

Our solution for the rotation period of 2005 UD:  $P = 5.224 \pm 0.003$  h and the light-curve amplitude of 0.34 mag is in the range of values reported by various publications (Jewitt & Hsieh 2006; Kinoshita et al. 2007; Devogèle et al. 2020; Huang et al. 2021; Kueny et al. 2023). Although statistically we could generate a three peak solution with a period of  $P = 7.851 \pm 0.001$  h and an amplitude of 0.37 mag, we excluded it as an alias. That is because according to Harris et al. (2014), for light curves determined at low phase angles with an amplitude greater than 0.4 mag, the dominance of higher order harmonics is unlikely, unless the spin is complex. In this case, we found the amplitude of the light curve to be close to the above-mentioned threshold. Moreover, it is very hard to envision an asteroid with irregular surface producing an almost perfect sinusoidal three-peaked period.

However, the high signal-to-noise ratio light curves obtained with INT show a general trend towards higher magnitudes (Fig. 3), where both maxima and minima seem to have higher magnitudes with time, with differences of at least 0.05 mag. The trend remains obvious even when accounting for the relatively small phase angle, distance, air mass, and zero-point offsets variations. We performed a dual

<sup>5</sup><https://alcdef.org/>

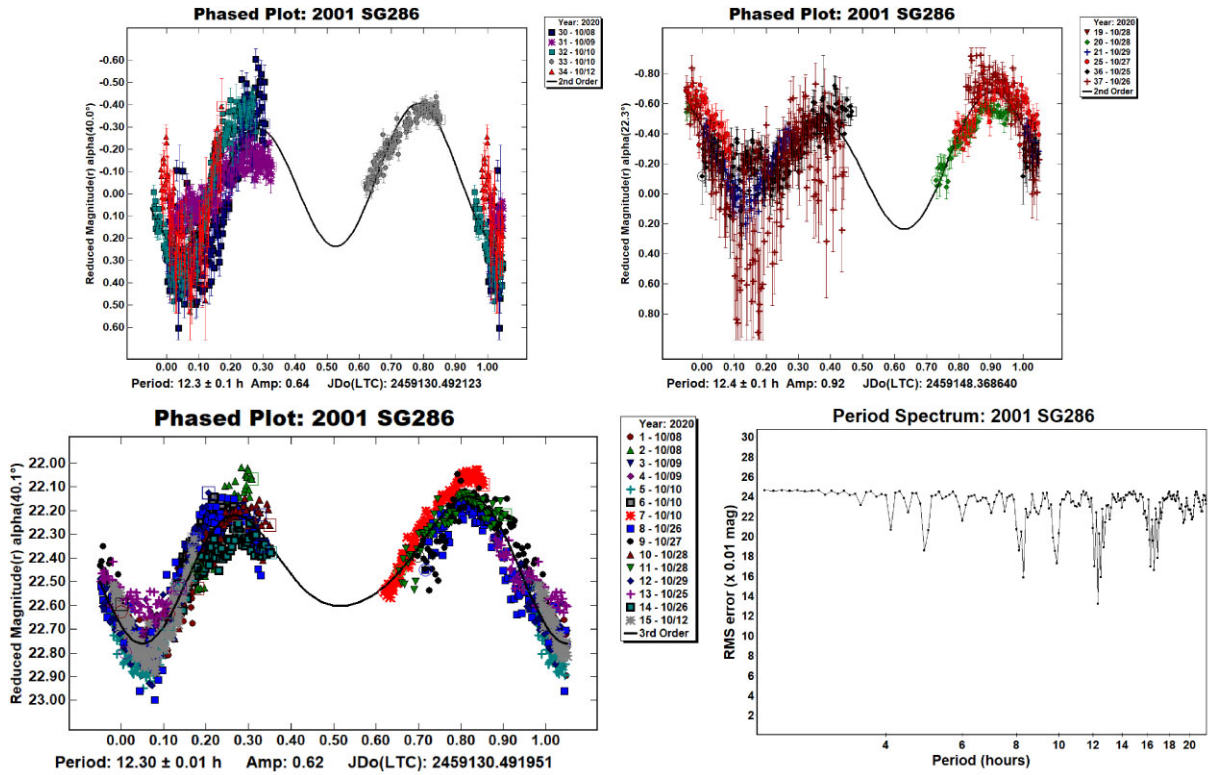


**Figure 2.** The light curve of 2001 SG286. On top, the phased curves resulted from each observing run, and on bottom, the complete phased curve (left) and its period spectrum (right), obtained with the INT/WFC instrument. The various observing sessions are plotted with a different colour.

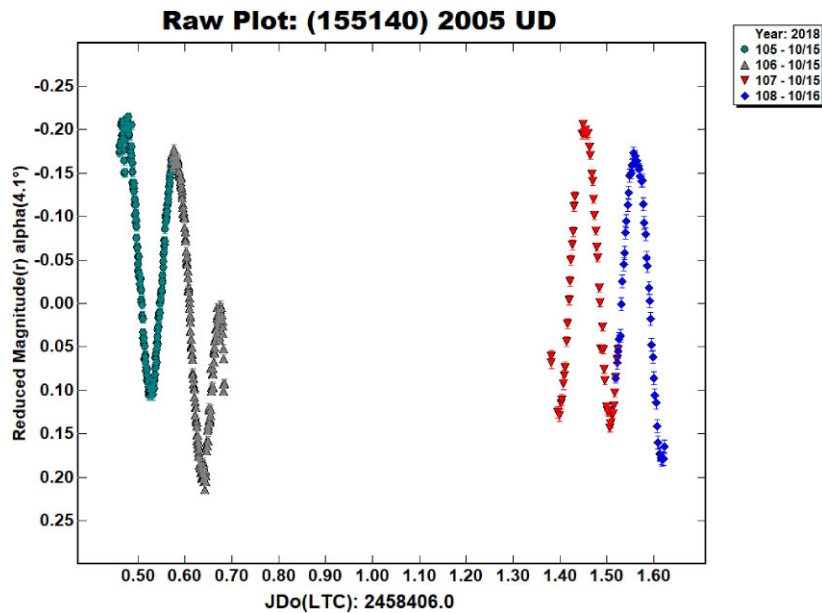


**Figure 3.** The raw magnitude variation of 2005 UD, with unity-distance and  $H-G$  phase correction applied ( $G = 0.15$ ). In this case, the high-quality INT data were selected for plotting. A secondary magnitude trend towards higher magnitudes can be noticed even during each nightly observing session where the phase angle variation was negligible under 0.5 deg.

period search using the available data from all the above-mentioned telescopes but without any conclusive result. Nevertheless, although there could still be a small observation bias due to the opposition effect, in our opinion this effect is better explained by a secondary,

larger periodic variation which might statistically favour other solution. Thus, we can argue for the existence of a secondary rotation axis with a longer period. In this case, we may speculate that 2005 UD has a double-period (tumbler) rotation, with  $P_1 = 5.23$  h and a much

longer (which we could not determine with our current limited data) P2. Jewitt & Hsieh (2006) also hypothesized a multiple axis rotation with similar observational results. If 2005 UD formed from a parent body as a result of a violent collision or break-up and it experienced material ejection, it may represent the origin of Sextantides meteor shower (Ohtsuka et al. 2005). This could also explain the secondary rotation axis.

*The spectrophotometry and spectroscopy at visible wavelengths.* The INT observations performed on the night of October 15 with different filters allowed us to determine the colour indices of (155140) 2005 UD. The following values were found:  $(g-r) = 0.42 \pm 0.01$  mag,  $(g-i) = 0.52 \pm 0.02$  mag, and  $(r-i) = 0.10 \pm 0.02$ . This result can be compared with the reflectance spectrum. To compare the spectral data with the spectrophotometric observations we converted the colour indices to reflectances. This was done using equation (1) (e.g. Popescu et al. 2018):

$$R_{\text{aster}}^{f1} / R_{\text{aster}}^{f2} = 10^{-0.4(C_{f1-f2} - C_{f1-f2}^{\text{Sun}})} \quad (1)$$

The  $f1$  and  $f2$  are two different filters, the corresponding colour is  $(C_{f1-f2}$  and  $C_{f1-f2}^{\text{Sun}}$ ) represent the colour of the Sun, and  $R_{\text{aster}}^{f1}$  and  $R_{\text{aster}}^{f2}$  are the asteroid reflectances. The following colours of the Sun were used (Holmberg, Flynn & Portinari 2006) for the Sloan Digital Sky Survey (SDSS) filters  $(g-r)^{\text{Sun}} = 0.45 \pm 0.02$  mag and  $(r-i)^{\text{Sun}} = 0.12 \pm 0.01$  mag. Finally, we normalized the reflectances at the  $r$  filter ( $R_{\text{aster}}^r = 1$ ).

Fig. 4 shows the comparison between the average spectrum obtained on 2020 October 17 with INT/IDS and the spectrophotometric values obtained with INT/WFC on 2020 October 15. The matching between the two sets of data obtained with different setups gives confidence in the obtained results. We notice a slight turn up of the spectrum above  $0.75 \mu\text{m}$  which might be an artefact due to fringing effect or due to the second-order contamination. During the night of 2018 October 17, we obtained 17 consecutive visible spectral exposures of 10 min each. There is a slight variation of spectral slope between these exposures, however we found that this is correlated with the airmass. We did not find any spectral variation between the observations outside the error bars of the obtained data ( $1\sigma$ ), indicating that there is no large composition heterogeneity.

*The thermal excess.* The near-infrared spectrum of 2005 UD shows a considerable amount of thermal emission in the near-infrared, even though at the time of the observation the asteroid was at distance of 1.55 au from the Sun. We calculated the thermal excess according to the thermal model described by Rivkin, Binzel & Bus (2005):

$$\gamma = \frac{T_{2.5}}{R_{2.5}}, \quad (2)$$

where  $R_{2.5}$  is the reflected flux at  $2.5 \mu\text{m}$ , determined by extrapolating a linear continuum from shorter wavelengths ( $2.1 \mu\text{m}$ ) to  $2.5 \mu\text{m}$  (Fig. 5) and  $T_{2.5}$  is the thermal flux at  $2.5 \mu\text{m}$ . The resulting thermal excess value is  $0.42 \pm 0.16$ .

By applying Rivkin et al. (2005) model and taking into account the heliocentric distance of the object at the time of the observation, we determined the geometrical albedo of 2005 UD to be  $p_V = 0.06 \pm 0.02$ . This result is similar to the most recent estimate of Masiero et al. (2020),  $p_V = 0.054 (+0.036/-0.022)$ , but at the lower limit compared to the result of Devogèle et al. (2020), where  $p_V = 0.10 \pm 0.02$ . In the latter case, their value was determined using the albedo-polarization relation. The differences between the values reported by various authors may be due to underestimated uncertainties in the different methods used (e.g. uncertainty in the absolute magnitude).

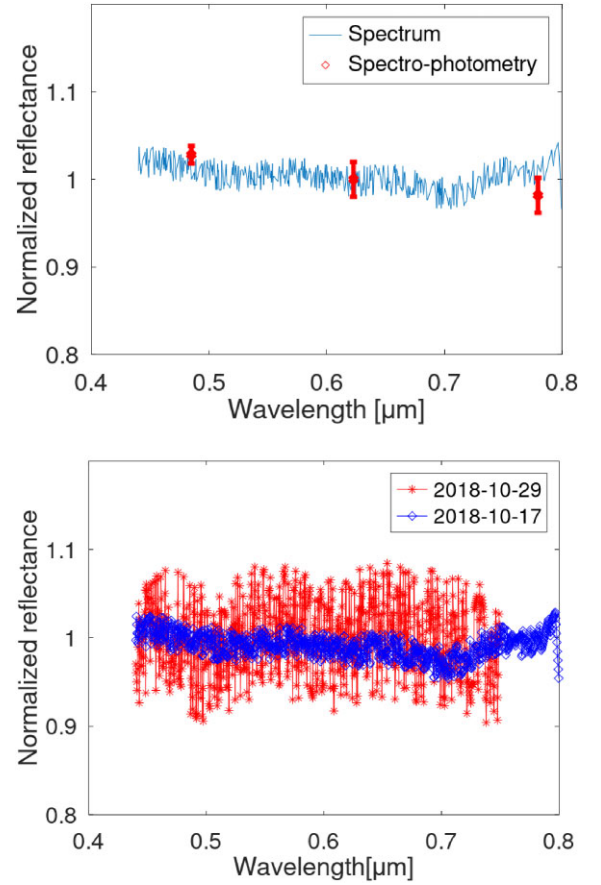


**Figure 4.** Top: the comparison between the average spectrum of 2005 UD obtained on October 17, and its reflectances determined using broad-band filters. Bottom: comparison between the spectra of 2005 UD obtained at different dates.

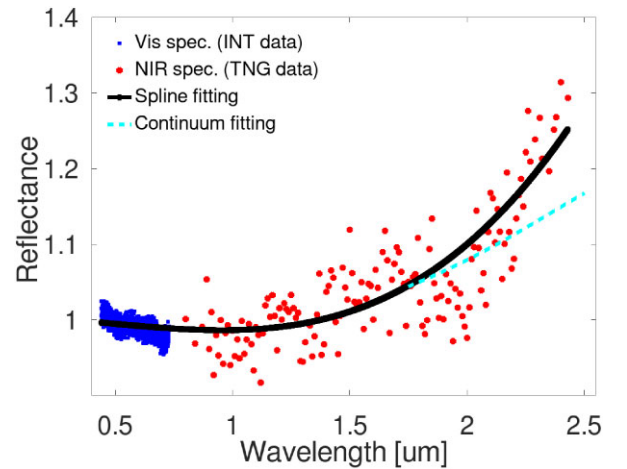


**Figure 5.** 2005UD: the thermal excess at the near-infrared wavelengths.

By using the above-determined albedo and the value currently found in the literature for the absolute magnitude  $H = 17.51 \pm 0.02$  (Devogèle et al. 2020), we determined the diameter of 2005 UD to be  $D = 1.7 \pm 0.3$  km according to the relation (3) below (Harris & Harris 1997):

$$\log_{10} D = 3.1236 - 0.2H - 0.5 \log_{10} p_V. \quad (3)$$

**Taxonomic classification.** We merged the average visible spectrum obtained on 2018 October 17 with the near-infrared one obtained with TNG on 2018 October 31. Although 2005 UD presents a slightly blue slope in the visible region, it turns in the near-infrared part. The best curve match for this is the Cb type from Bus–DeMeo taxonomy (DeMeo et al. 2009). This classification differs from the one proposed by Devogèle et al. (2020), who identified it as B type based on a visible spectrum. Kareta et al. (2021) obtained the near-infrared spectra of 2005 UD during 2018 October 2 and 3 using the 3.0-m NASA Infrared Telescope Facility. The overall 0.8–2.5  $\mu\text{m}$  spectral trend is similar with ours, except the thermal excess. This confirms our Cb-type classification (Fig. 6).

Jewitt & Hsieh (2006) suggested that 2005 UD might be a fragment of (3200) Phaeton – the parent body of the Geminid meteor stream. This assumption was proposed based on orbital similarities. Another association between 2005 UD and Daytime Sextantids was made by Dumitru et al. (2017), by using three D-Criteria metrics and their own method of threshold selection, from which two metrics found similarities: Southworth and Hawkins (1963) metric – 0.1521 and Jopek (1993) metric – 0.1595. Also, they concluded that 2005 UD may be a long-time contributor to the meteor shower due to its stable orbit (Lyapunov time – 478). The orbital evolution was made for 10 clones on a period of 10 000 yr backward in time and the Lyapunov time for 2000 yr. The spectral and the spectrophotometric data obtained over the visible wavelengths supported this hypothesis. Nevertheless, by analysing the orbital similarity and minimum orbit intersection distance over the last 5000 yr, Ryabova et al. (2019) argue that 2005 UD is not a member of Phaeton–Geminid complex.

Our observations performed with TNG show a positive slope in the near-infrared for 2005 UD which is indicative of potentially different surface properties when comparing with the spectrum of (3200) Phaeton. Phaeton appears to have a slightly higher geometric albedo with estimates ranging from 0.09 to 0.12 (Ito et al. 2018) and a steeper blue slope fitting in the B-type category in the Bus–DeMeo taxonomy (Licandro et al. 2007), while also having a negative slope in the near infrared part of the spectrum.

A sample of 45 B types classified only based on visible data were observed by de León et al. (2012) at near-infrared wavelengths. They found a continuous shape variation of the near-infrared (0.8–2.5  $\mu\text{m}$ ) spectral curves. It varies from a monotonic negative (blue) slope to a positive (red) slope. While all of them are matching the carbonaceous chondrites spectra, there is also progressive change in composition that correlates with the spectral slope, from CM2 chondrites (water-rich, aqueously altered) corresponding to the reddest group, to CK4 chondrites (dry, heated/thermally altered) for the bluest one. We determined that the visible to near-infrared (VNIR) spectrum and the albedo of 2005 UD is similar with that of the group G3 defined by León et al. (2012). For comparison, these authors placed (3200) Phaeton in group G6.

MacLennan, Toliou & Granvik (2021) found likely (based on orbital integration) that 2005 UD originated in the inner part of the asteroid belt in the families (329) Svea or (142) Polana. We outline a similar VNIR spectral trend of 2005 UD and (142) Polana (León et al. 2012).

**Comparison with laboratory spectra.** The surface characteristics of asteroids can also be derived by comparing their remotely acquired spectrum with a catalogue of meteorite spectra. While this process still presents challenges (Miyamoto et al. 2018), careful analysis of statistically relevant similarities in spectral features can still provide an useful insight into the surface properties of nearby small planetary

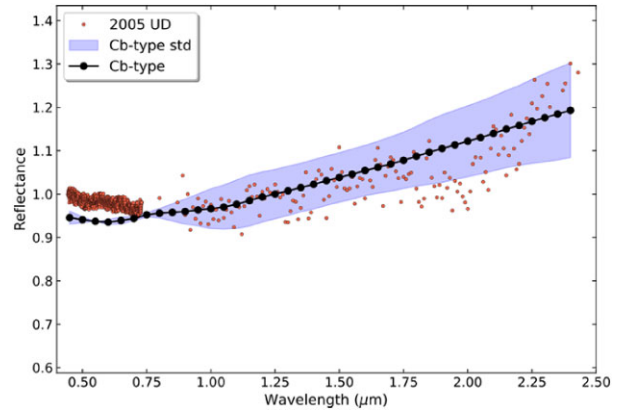


**Figure 6.** The match between the Cb spectral template and the visible to near-infrared spectrum of 2005 UD.

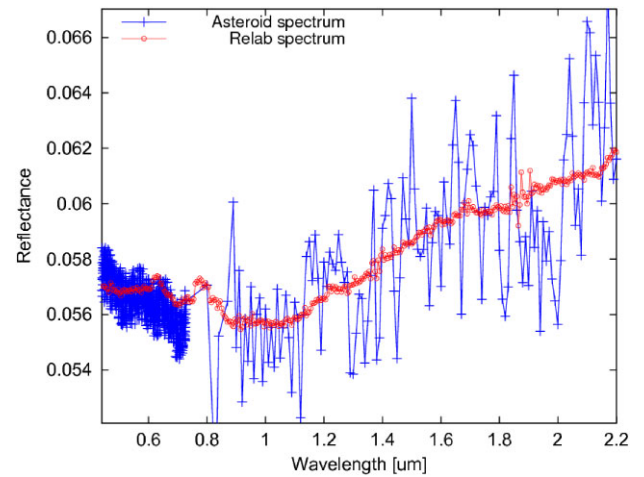


**Figure 7.** Comparison of 2005 UD spectrum with the Relab spectrum. The spectrum of the asteroid was normalized to its median value and then multiplied with the median value of the Relab spectrum.

bodies. Thus, we employed the M4Ast tool (Popescu et al. 2011) to compare the 2005 UD spectrum with meteorite laboratory spectra in an attempt to determine its mineralogy. M4Ast uses sparse modelling in order to find the closest analogue among the meteorite spectra from the Relab database<sup>6</sup> (Pieters & Hiroi 2004; Milliken, Hiroi & Patterson 2016).

As seen in Fig. 7, the 2005 UD spectrum fits best with a CM2 carbonaceous chondrite meteorite spectrum sample heated at 900 °C, with a mean square coefficient of 0.00113. Similarly, at perihelion, the subsolar equilibrium surface temperature of 2005 UD reaches above 300 °C or 600 K (Burbine et al. 2009). In these conditions, phenomena such as surface thermal stress and fracturing along with desiccation of hydrated minerals are common. This is an evidence that 2005 UD is a Cb-type asteroid with thermally metamorphosed CM/CI mineralogy and generally fine-grained surface.

#### 4.2 2001 SG286

**The light curves.** The observations performed with INT span a time interval of 22 nights and were obtained during nine sessions. The S/N

<sup>6</sup><https://sites.brown.edu/rehab/rehab-spectral-database/>



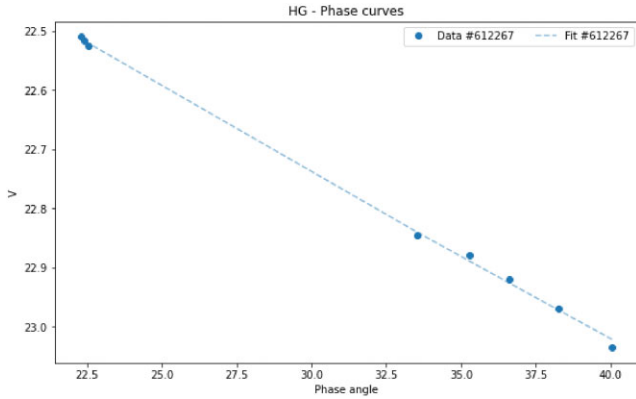


Figure 8.  $H$ - $G$  phase curve diagram of 2001 SG286.

ratio varied due to the presence of the Moon and other environmental factors. The Fourier period spectrum shows several peaks, the most prominent one corresponds to a rotation period of  $12.3 \pm 0.01$  h. The folded light curve has an amplitude of 0.62 mag and is shown in Fig. 2.

The photometry data were taken during several weeks while the asteroid had a high relative movement and different phase angles, thus we were able to determine the linear part of its phase curve. We could not acquire data corresponding to lower phase angles because the minimum observable phase angle during the 2020 apparition was about  $22^\circ$ . Moreover, as the nightly light-curve data could not cover the whole rotation period of 12.3 h, we used the Fourier analysis method of the composite light-curve spanning groups of adjacent two nights in order to minimize the phase angle dependence for the determination of the amplitude corroborated with the raw data for the computation of the mean level of brightness expressed in reduced magnitude  $r$  during each observing nightly session. The observation log (Table 2) shows that the phase angle did not have a significant nightly variation, and the observations were carried out for as long as possible at once on many consecutive nights. For each nightly observation session, we took into account the average phase angle value due to the small corresponding variation.

Since the  $H$  magnitude is defined in the Johnson  $V$  filter band and our observations were carried out in the Sloan  $r$  filter, we converted our values first to the Johnson  $R$  system and finally to the  $V$  system by using the relation described in Jordi, Grebel & Ammon (2006):

$$R = -0.267(V - R) - 0.088 + r. \quad (4)$$

The colour index  $V - R$  was calculated from the spectral data by integrating the observed flux densities over the wavelength range consistent with the bandpass and relative response profile of both Johnson  $V$  and  $R$  standards and subsequently using the magnitude–flux relationship:

$$m_V - m_R = -2.5 \log_{10} \frac{F_V}{F_R}. \quad (5)$$

The resulted  $V - R$  colour is  $0.55 \pm 0.05$ .

With the  $V$  magnitudes now known, we applied the PYEDRA software routine (Colazo et al. 2021) and the online calculator for  $H$ ,  $G_1$ , and  $G_2$  photometric system using non-linear, constrained fit (Penttilä et al. 2016) for the  $H$ - $G$  and  $H$ - $G_1G_2$  functions, respectively (Fig. 8 and 9). We estimate the value for the absolute magnitude of 2001 SG286 at  $H(0) = 21.4 \pm 0.3$ , with the slope parameters  $G = 0.16 \pm 0.04$ ,  $G_1 = 0.66$ , and  $G_2 = 0.24$ . While still presenting some uncertainty due to the lack of data at low phase angles during the

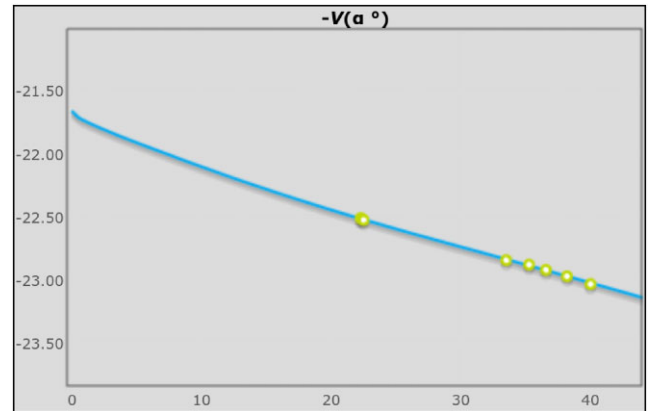


Figure 9.  $H$ - $G_1G_2$  diagram of 2001 SG286.

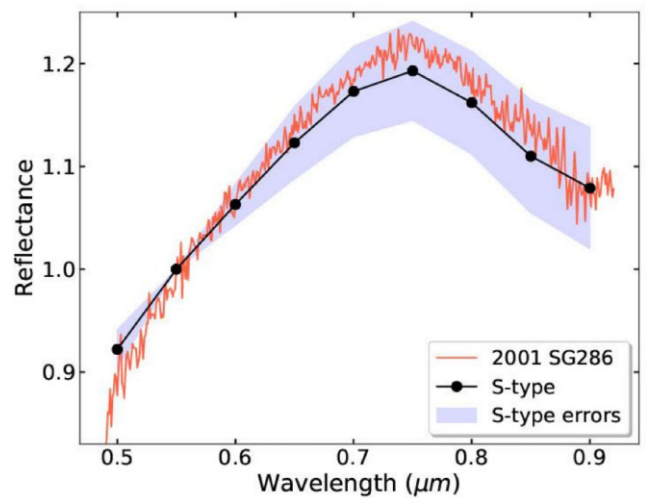


Figure 10 2001 SG286 optical spectrum.

opposition surge and the faintness of this target, these result is close to the latest estimate currently found in the literature:  $H(0) = 21.1$  (Binzel et al. 2004).

The accurate visible spectrum 2001 SG286 obtained with GTC is clearly consistent with an S-type taxonomic classification, according to Bus–DeMeo taxonomy. It has the peak reflectance at the 730-nm wavelength (Fig. 10) and the drop-off corresponding to the 1- $\mu$ m band characteristic for olivine–pyroxene compositions. These new high-quality data are not in agreement with the previous reports in the literature (Binzel et al. 2004; Popescu et al. 2011). The low signal-to-noise ratio spectra presented by these authors indicated a possible D-type classification due to the fact that the 1- $\mu$ m band was hidden in the noise.

Furthermore, the  $G$  slope parameter value is typical for an S-type asteroid (Vereš et al. 2015). The S-type classification makes 2001 SG281 a less peculiar object than considered before. By assuming a typical albedo of 0.20 for S-type asteroids, we can also infer the mean diameter of 2001 SG286 at  $0.16 \pm 0.03$  km.

## 5 CONCLUSIONS

The space exploration of minor bodies relies on the prior information we can acquire with the ground-based telescopes. Typically, the favourable observing geometries for most of the NEAs are during 2–

4 weeks, once per decade. An observing campaign made with various telescopes can provide the physical properties critical for planning a space mission.

In this article, we presented the results obtained for (155140) 2005 UD, which is a potential target for *DESTINY+* mission, and for (612267) 2001 SG286 which has been considered as candidate for space exploration thanks to its low  $\Delta - V$  budget and peculiar properties. For each of these two objects we made an observing campaign using the 0.46 m TAR2, the 2.54 m INT, the 3.58 m TNG, and the 10.4 m GTC. The data were obtained during 2018 October for 2005 UD and 2020 October for 2001 SG286.

The best solution for 2005 UD is a double-peaked light curve with a rotation period of  $5.234 \pm 0.001$  with an amplitude of 0.34 mag. However, we also identified with the INT data, a likely trend towards higher amplitudes which may indicate a secondary rotation axis with a larger period. This possibility has been previously reported by Jewitt & Hsieh (2006) and further high-quality observations are needed to confirm it.

The visible to near-infrared spectrum of 2005 UD was obtained with the INT and the TNG telescopes. The merged spectral curve covers the 0.4–2.45  $\mu\text{m}$  wavelengths. The spectral observations performed during three nights with INT/IDS spectrograph shows no variation outside the error bars. The visible spectral shape of 2005 UD was also confirmed using the spectrophotometric data obtained with *g*, *r*, and *i* Sloan filters. These observations were made with the INT.

We classified 2005 UD as a Cb type in Bus–DeMeo (DeMeo et al. 2009). We estimated its albedo as  $p_V = 0.06 \pm 0.02$  using the thermal emission flux at 2.5  $\mu\text{m}$ . By comparing the spectral curve with those of meteorites reported in Relab spectral database, we found a matching with heated carbonaceous chondrite meteorites of CM2 type. We also report significant differences in the spectrum of 2005 UD compared to that of (3200) Phaeton, the latter being previously suggested as its parent body based on dynamical similarities.

The accurate visible spectrum obtained with the GTC shows that 2001 SG286 is an S-type asteroid in in Bus–DeMeo (DeMeo et al. 2009) taxonomic system. The photometric data obtained with INT indicate a rotation period of  $12.30 \pm 0.01$  h and an amplitude of 0.64 mag. With these observations we also estimated its absolute magnitude  $H = 21.4 \pm 0.3$ , thus allowing to estimate its size as  $160 \pm 45$  m. According to our results, 2001 SG286 appears to be a small diameter slow rotator.

## ACKNOWLEDGEMENTS

We thank the director of the Telescopio Nazionale Galileo for allocation of Director’s Discretionary Time. This project has received funding from the European Union’s Horizon 2020 research and innovation program under grant agreement no. 870403 (NEOROCKS). The work of RMG, MP, and BD was supported by a grant of the Romanian National Authority for Scientific Research and Innovation, CNCS–UEFISCDI, project no. PN-III-P1-1.1-TE-2019-1504. The work of MP and OV was also partially supported by a grant of the Romanian National Authority for Scientific Research – UEFISCDI, project no. PN-III-P2-2.1-PED-2021-3625.

## DATA AVAILABILITY

Data available on request. The data underlying this article will be shared on reasonable request to the corresponding author.

## REFERENCES

- Baffa C. et al., 2001, *A&A*, 378, 722  
 Barucci M. A. et al., 2018, *MNRAS*, 476, 4481  
 Bertin E., 2006, in Gabriel C., Arviset C., Ponz D., Enrique S. eds, ASP Conf. Ser. Vol. 351, *Astronomical Data Analysis Software and Systems XV*, p. 112  
 Bertin E., Arnouts S., 1996, *A&AS*, 117, 393  
 Bertin E., Mellier Y., Radovich M., Missonnier G., Didelon P., Morin B., 2002, in Bohlender D. A., Durand D., Handley T. H. eds, ASP Conf. Ser. Vol. 281, *Astronomical Data Analysis Software and Systems XI*, p. 228  
 Binzel R., Perozzi E., Rivkin A., Rossi A., Harris A., Bus S., Valsecchi G., Slivan S., 2004, *Meteorit. Planet. Sci.*, 39, 351  
 Burbine T. H., Buchanan P. C., Dolkar T., Binzel R. P., 2009, *Meteorit. Planet. Sci.*, 44, 1331, <https://doi.org/10.1111/j.1945-5100.2009.tb01225.x>  
 Cepa J. et al., 2000, in Iye M., Moorwood A. eds, *Proc. SPIE Conf. Ser. Vol. 4008, Optical and IR Telescope Instrumentation and Detectors*, p. 623  
 Cepa J., 2010, in *Highlights of Spanish Astrophysics V*, p. 15  
 Colazo M. R., Cabral J. B., Chalela M., Sánchez B. O., 2021, *Astrophysics Source Code Library*, record ascl:2103.008  
 de León J., Pinilla-Alonso N., Campins H., Licandro J., Marzo G. A., 2012, *Icarus*, 218, 196  
 DeMeo F. E., Binzel R. P., Slivan S. M., Bus S. J., 2009, *Icarus*, 202, 160  
 Devogèle M. et al., 2020, *Planet. Sci. J.*, 1, 15  
 Dumitru B. A., Birlan M., Popescu M., Nedelcu D. A., 2017, *A&A*, 607, A5  
 Eaton J., Bateman D., Hauberg S., 2015, *The GNU Octave 4.0 Reference Manual 1/2: Free Your Numbers*. Samurai Media Limited, <https://books.google.ro/books?id=cIz8jgEACAAJ>  
 Flewelling H. A. et al., 2020, *ApJS*, 251, 7  
 Gaia Collaboration, 2018, *A&A*, 616, A1  
 Harris A. et al., 1989, *Icarus*, 77, 171, [https://doi.org/10.1016/0019-1035\(89\)90015-8](https://doi.org/10.1016/0019-1035(89)90015-8)  
 Harris A. et al., 2014, *Icarus*, 235, 55, <https://doi.org/10.1016/j.icarus.2014.03.004>  
 Harris A. W., Harris A. W., 1997, *Icarus*, 126, 450, <https://doi.org/10.1006/icar.1996.5664>  
 Holmberg J., Flynn C., Portinari L., 2006, *MNRAS*, 367, 449  
 Howell S. B., 2000, *Handbook of CCD Astronomy*. Cambridge University Press  
 Huang J. N., Muinonen K., Chen T., Wang X. B., 2021, *Planet. Space Sci.*, 195, 105120  
 Ito T. et al., 2018, *Nat. Commun.*, 9, 2486  
 Jewitt D., Hsieh H., 2006, *AJ*, 132, 1624  
 Jopek (1993) *Icarus*, 603, 00191035  
 Jordi K., Grebel E. K., Ammon K., 2006, *A&A*, 460, 339  
 Kareta T., Reddy V., Pearson N. C., Sanchez J. A., Harris W. M., 2021, *Planet. Sci. J.*, 2  
 Kasuga T., 2009, *Earth Moon Planets*, 105, 321  
 Kinoshita D. et al., 2007, *A&A*, 466, 1153  
 Kueny J. et al., 2023, *Planet. Sci. J.*, 4, 56  
 Lauretta D. S. et al., 2019, *Nature*, 568, 55  
 Licandro J., Campins H., Mothé-Diniz T., Pinilla-Alonso N., De León J., 2007, *A&A*, 461, 751  
 MacLennan E., Toliou A., Granvik M., 2021, *Icarus*, 366, 114535  
 Masiero J. R., Smith P., Teodoro L. D., Mainzer A. K., Cutri R. M., Grav T., Wright E. L., 2020, *Planet. Sci. J.*, 1, 9  
 Masiero J. R., Wright E. L., Mainzer A. K., 2019, *AJ*, 158, 97  
 Medeiros H. et al., 2019, *MNRAS*, 488, 3866  
 Milliken R. E., Hiroi T., Patterson W., 2016, *LPI Contrib.*, 2058  
 Miyamoto H. et al., 2018, *J. Phys.: Conf. Ser.*, 1036, 012003  
 Mommert M., 2017, *Astron. Comput.*, 18, 47  
 Morate D., de León J., De Prá M., Licandro J., Cabrera-Lavers A., Campins H., Pinilla-Alonso N., Alí-Lagoa V., 2016, *A&A*, 586, A129  
 Nakamura T. et al., 2023, *Science*, 379, abn8671  
 Ohtsuka K., Sekiguchi T., Kinoshita D., Watanabe J. I., Ito T., Arakida H., Kasuga T., 2006, *A&A*, 450, L25

- Ohtsuka K., Sekiguchi T., Kinoshita D., Watanabe J., 2005, Central Bureau Electronic Telegrams, 283, 1
- Ozaki N. et al., 2022, *Acta Astronaut.*, 196, 42
- Penttilä A., Shevchenko V., Wilkman O., Muinonen K., 2016, *Planet. Space Sci.*, 123, 117 <https://doi.org/10.1016/j.pss.2015.08.010>
- Pieters C. M., Hiroi T., 2004, in Mackwell S., Stansbery E.eds, LPI Contrib., 1720
- Popescu M. et al., 2019, *A&A*, 627, A124
- Popescu M., Birlan M., Binzel R., Vernazza P., Barucci A., Nedelcu D. A., DeMeo F., Fulchignoni M., 2011, *A&A*, 535, A15
- Popescu M., Licandro J., Carvano J. M., Stoicescu R., de León J., Morate D., Boacă I. L., Cristescu C. P., 2018, *A&A*, 617, A12
- Rivkin A. S., Binzel R. P., Bus S. J., 2005, *Icarus*, 175, 175
- Ryabova G. O., Avdyushev V. A., Williams I. P., 2019, *MNRAS*, 485, 3378
- Southworth R. B., Hawkins G. S. ; Statistics of meteor streams, Smithsonian Contributions to Astrophysics. vol 7, p.261-285
- Tody D., 1986, in Crawford D. L.ed., Proc. SPIE Conf. Ser. Vol. 627, Instrumentation in Astronomy VI, p. 733
- Vereš P. et al., 2015, *Icarus*, 261, 34
- Warner B. D., Stephens R. D., 2019, *Minor Planet Bull.*, 46, 144

This paper has been typeset from a  $\text{T}_{\text{E}}\text{X}/\text{L}_{\text{A}}\text{T}_{\text{E}}\text{X}$  file prepared by the author.